

Supporting Information

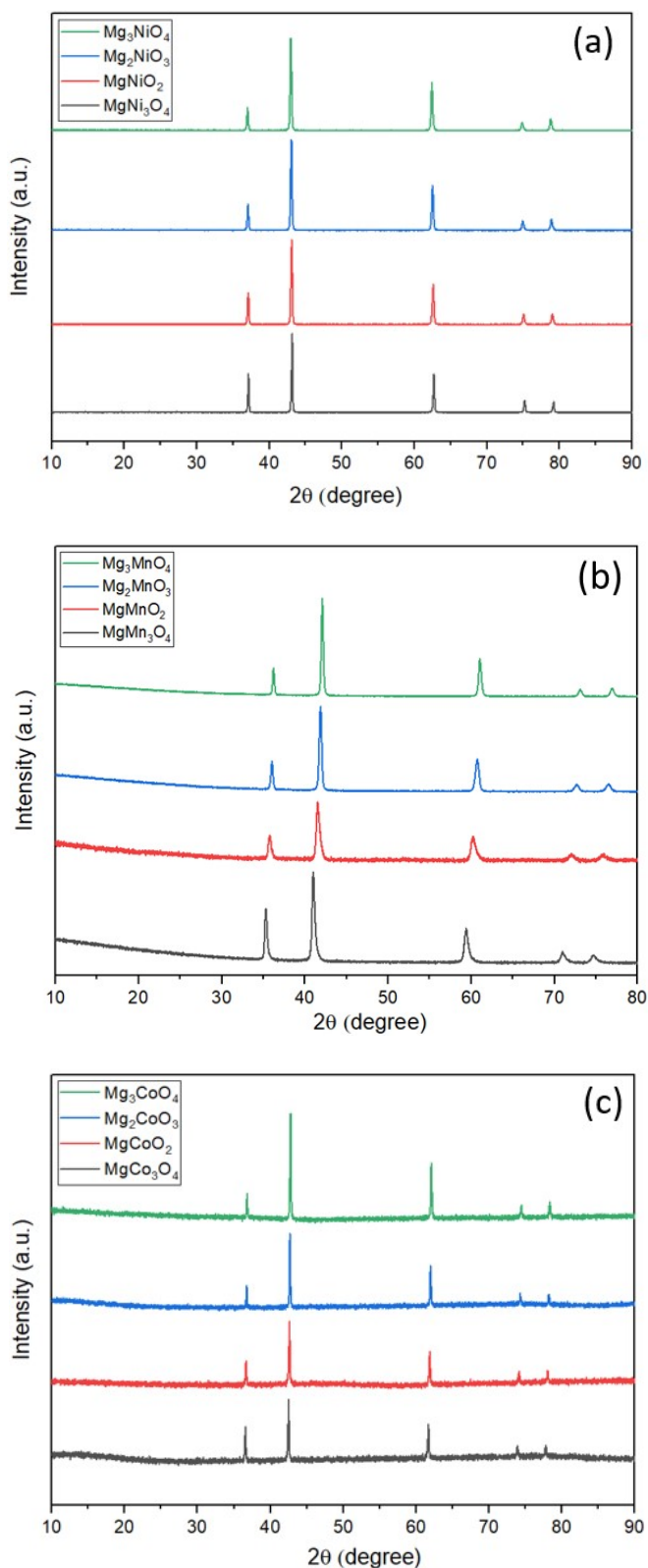


Fig. S1. Monochromatic PXRD data for as-synthesised (a) $\text{Mg}_x\text{Ni}_{1-x}\text{O}$, (b) $\text{Mg}_x\text{Mn}_{1-x}\text{O}$, and (c) $\text{Mg}_x\text{Co}_{1-x}\text{O}$ samples via solid-state method.

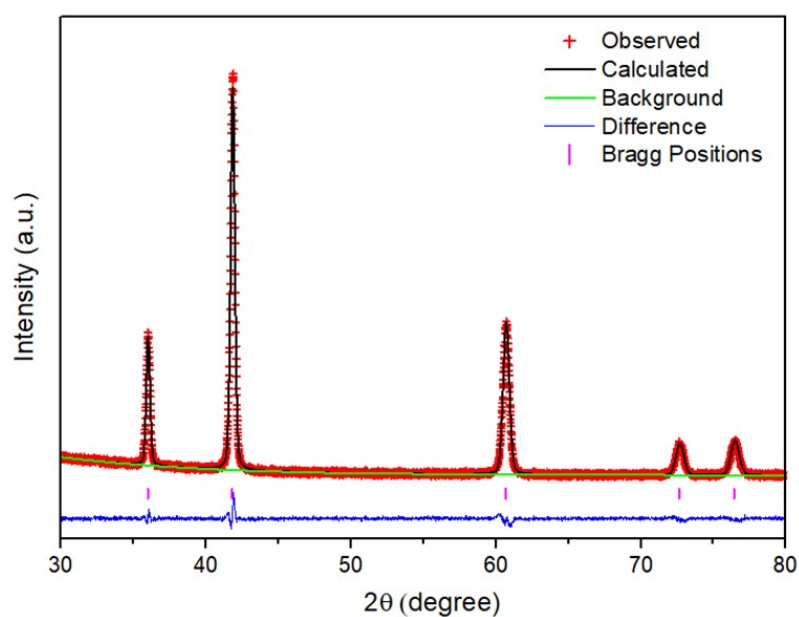


Fig. S2. Fitted XRD data for DRS Mg₂MnO₃ (before ball-milling) refined with Fm-3m space group.

Atom	Wyckoff Positions	x	y	z	Occupancy	U _{iso}
Mg	a	0	0	0	0.66	0.00977(4)
Mn	a	0	0	0	0.34	0.01267(4)
O	b	0.5	0.5	0.5	1	0.01479(3)
a=4.3054(3) Å, Space Group: Fm-3m, Domain size (μm)=1.0001, Microstrain=1081.2						
RF=1.057%, reduced $\chi^2=1.24$						

Table S1. Table of XRD Rietveld refinement parameters for Mg₂MnO₃ (before ball-milling).

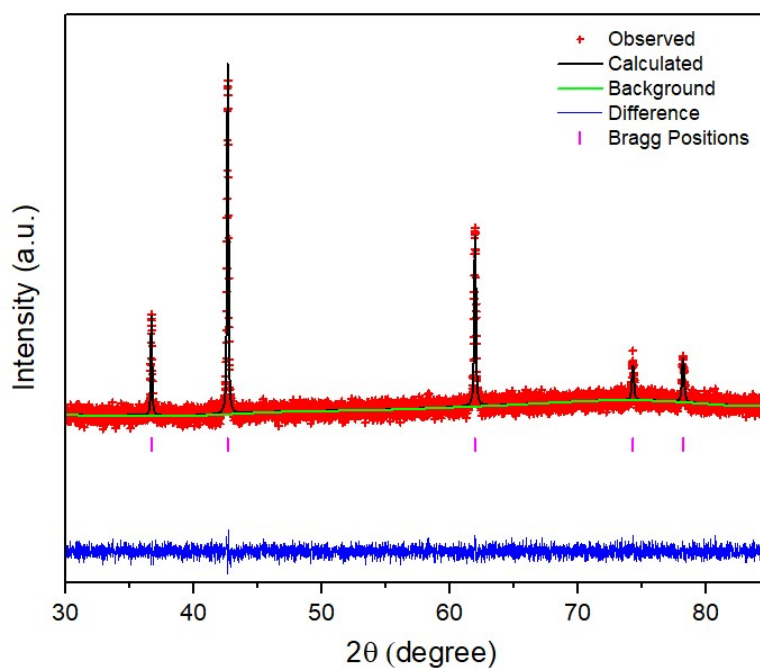


Fig. S3. Fitted XRD data for DRS Mg_2CoO_3 refined with Fm-3m space group.

Atom	Wyckoff Positions	x	y	z	Occupancy	U_{iso}
Mg	a	0	0	0	0.66	0.00122(1)
Co	a	0	0	0	0.34	0.00478(4)
O	b	0.5	0.5	0.5	1	0.00229(1)
a=4.2273(4) Å, Space Group: Fm-3m						
RF=24.231%, reduced $\chi^2=0.86$						

Table S2. Table of XRD Rietveld refinement parameters for Mg_2CoO_3 . It should be noted that the PXRD data for Co-containing compounds is noisy due to the high background fluorescence from Co.

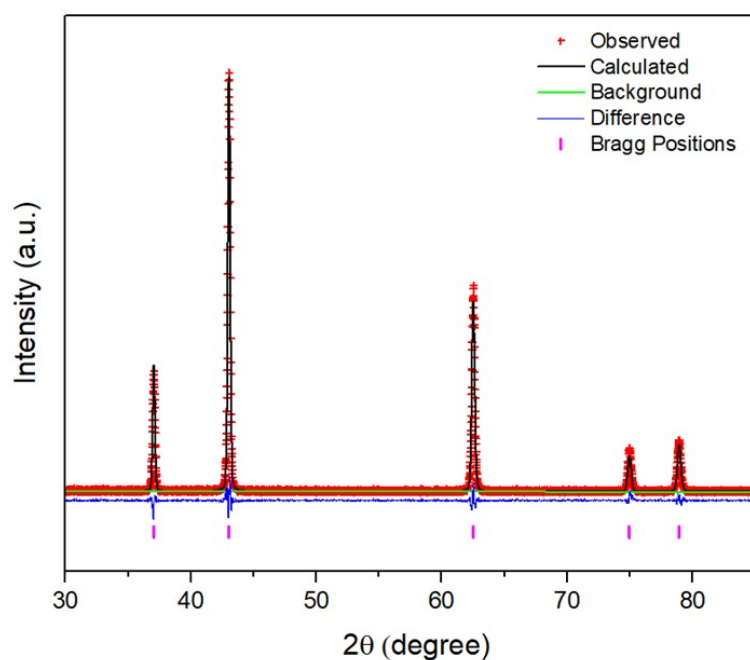


Fig. S4. Fitted XRD data for DRS Mg₂NiO₃ refined with Fm-3m space group.

Atom	Wyckoff Positions	x	y	z	Occupancy	U _{iso}
Mg	a	0	0	0	0.66	0.02085(6)
Ni	a	0	0	0	0.34	0.00070(6)
O	b	0.5	0.5	0.5	1	0.00551(1)

a=4.2041(7) Å, Space Group: Fm-3m
 RF=4.310%, reduced $\chi^2=1.00$

Table S3. Table of XRD Rietveld refinement parameters for Mg₂NiO₃.

Atom	Wyckoff	x	y	z	Occupancy
Mg	a	0	0	0	0.66
Mn	a	0	0	0	0.34
O	b	0.5	0.5	0.5	1
S.G.=Fm $\bar{3}$ m,		a=4.313 Å		$\alpha=90$	
R _w =0.207,					
Q _{max} =24 Å,					
r=1-40 Å,					

Table S4. X-ray PDF refinement parameters for Mg₂MnO₃ (without ball-milling).

Atom	Wyckoff	x	y	z	Occupancy
Mg	a	0	0	0	0.66
Co	a	0	0	0	0.34
O	b	0.5	0.5	0.5	1
S.G.=Fm $\bar{3}$ m,		a=4.230 Å		$\alpha=90$	
R _w =0.180,					
Q _{max} =24 Å,					
r=1-40 Å,					

Table S5. X-ray PDF refinement parameters for Mg₂CoO₃.

Atom	Wyckoff	x	y	z	Occupancy
Mg	a	0	0	0	0.66
Ni	a	0	0	0	0.34
O	b	0.5	0.5	0.5	1
S.G.=Fm $\bar{3}$ m,		a=4.196 Å		$\alpha=90$	
R _w =0.191,					
Q _{max} =24 Å,					
r=1-40 Å,					

Table S6. X-ray PDF refinement parameters for Mg₂NiO₃.

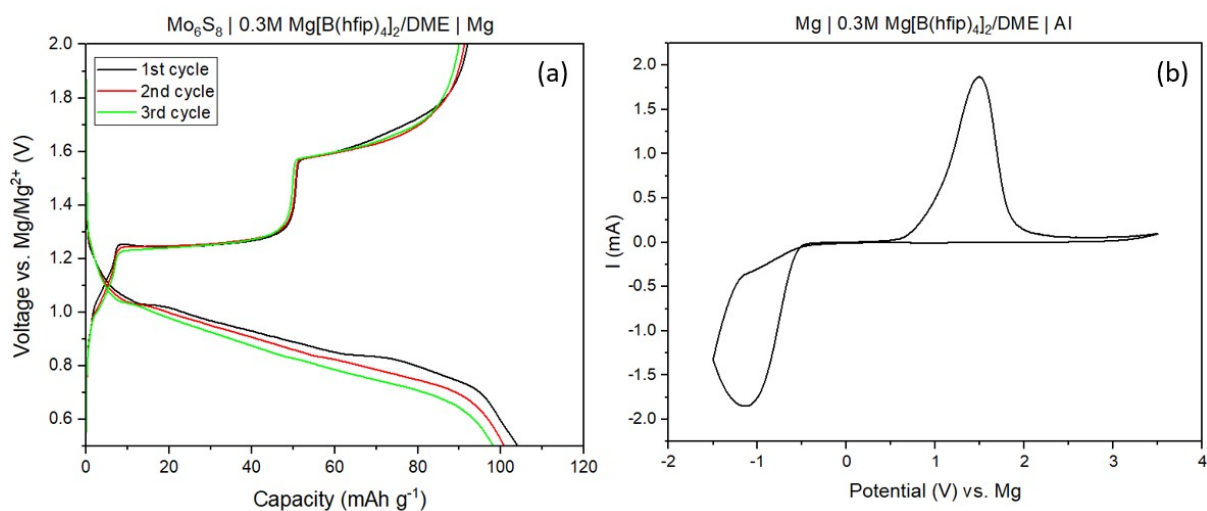


Fig. S5. (a). Galvanostatic discharge/charge profile of a $\text{Mo}_6\text{S}_8||\text{Mg}$ cell at 60°C using the $0.3\text{ M Mg}[\text{B}(\text{hfip})_4]_2$ in DME electrolyte, which shows comparable capacity to reported results.^{26,32} **(b) Cyclic voltammograms** using Al as the working electrode and Mg as the reference at a scan rate of 25 mV s^{-1} , and the profile reveals the $0.3\text{ M Mg}[\text{B}(\text{hfip})_4]_2/\text{DME}$ electrolyte is stable to at least 3.5 V vs. Mg in standard coin cells.

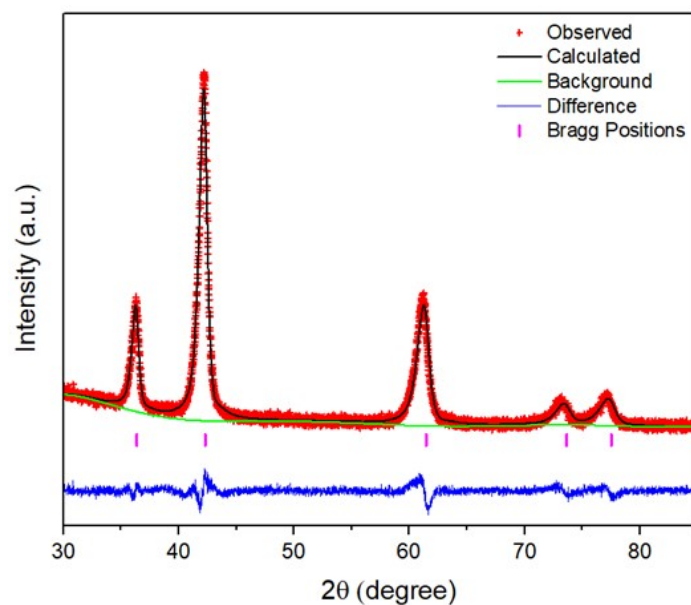


Fig. S6. Fitted XRD data for Mg_2MnO_3 after ball-milling at 200 rpm refined with Fm-3m space group.

Atom	Wyckoff Positions	x	y	z	Occupancy	U_{iso}
Mg	a	0	0	0	0.66	0.04190(2)
Mn	a	0	0	0	0.34	0.01434(3)
O	b	0.5	0.5	0.5	1	0.0002(0)
a=4.1970(8), Space Group: Fm-3m, Domain size (μm)=0.0389, Microstrain=2110.3						
RF=1.628%, reduced $\chi^2=1.58$						

Table S7. Table of XRD Rietveld refinement parameters for Mg_2MnO_3 after ball-milling at 200 rpm. The domain size is noted to be much reduced compared to the sample before ball-milling, accompanied by an increased degree of strain effects.

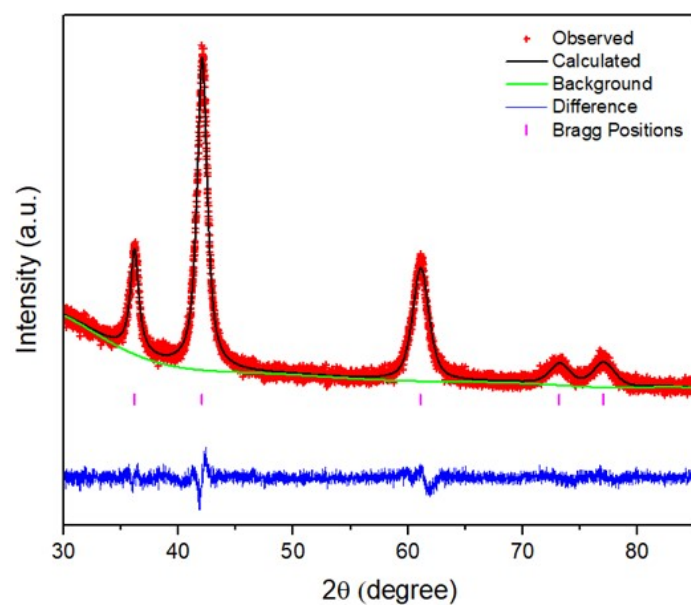


Fig. S7. Fitted XRD data for Mg_2MnO_3 after ball-milling at 300 rpm refined with Fm-3m space group.

Atom	Wyckoff Positions	x	y	z	Occupancy	U_{iso}
Mg	a	0	0	0	0.66	0.04397(2)
Mn	a	0	0	0	0.34	0.00007(9)
O	b	0.5	0.5	0.5	1	0.01789(4)
a=4.2298(8), Space Group: Fm-3m, Domain size (μm)=0.0168, Microstrain=2531.6						
RF=1.582%, reduced $\chi^2=1.09$						

Table S8. Table of XRD Rietveld refinement parameters for Mg_2MnO_3 after ball-milling at 300 rpm. The domain size is noted to be smaller compared to that of Mg_2MnO_3 after ball-milling at 200 rpm and the sample before ball-milling, whereas the microstrain is the highest.

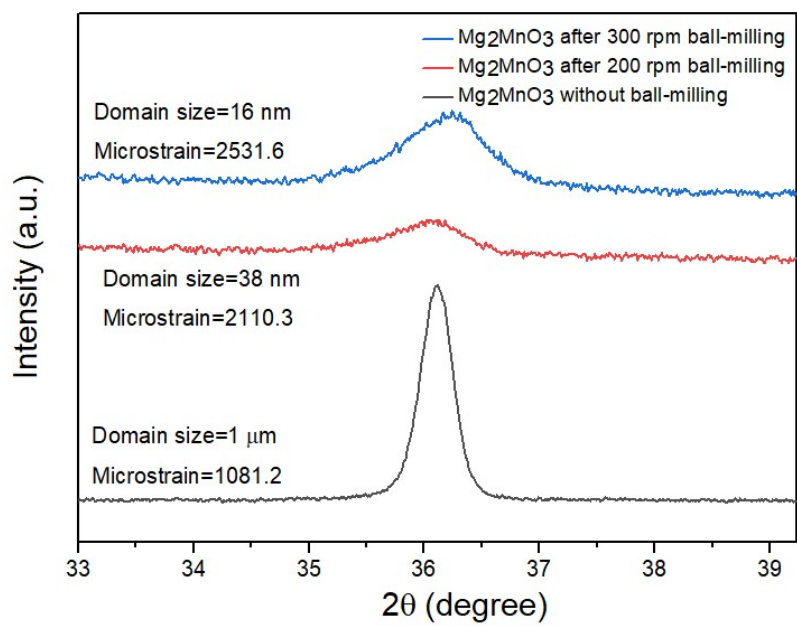


Fig. S8. PXRD patterns of Mg₂MnO₃ showing the shift in (111) peak to higher scattering angle and peak broadening after ball-milling.

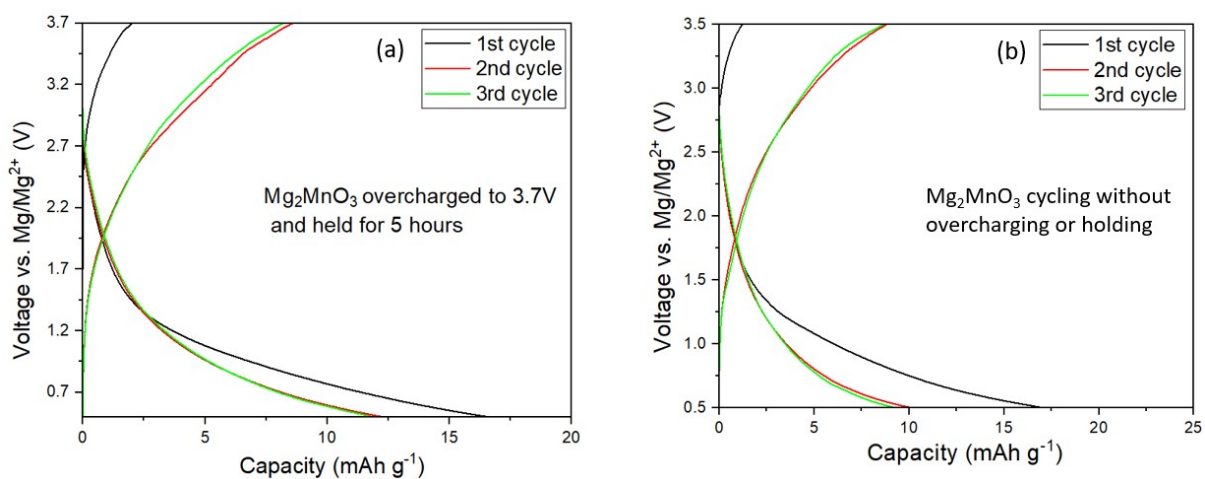


Fig. S9. Charge/discharge profiles of Mg_2MnO_3 after ball-milling at 300 rpm at 60°C and at a current density of 10 mA g⁻¹. The cathode was overcharged to 3.7V and held for 5 hours as an attempt to force it to de-magnesiate.